

Evaluating two methods of estimating error variances using simulated data sets with known errors

Therese Rieckh^{1,2} and Richard Anthes¹

¹COSMIC Program Office, University Corporation for Atmospheric Research, Colorado, U.S.A.

²Wegener Center for Climate and Global Change, University of Graz, Graz, Austria

Correspondence: Richard Anthes (anthes@ucar.edu)

Abstract. In this paper we compare two different methods of estimating the error variances of two or more independent data sets. One method, called the “three-cornered hat” (3CH) method, requires three data sets. Another method, which we call the “two-cornered hat” (2CH) method, requires only two data sets. Both methods have been used in previous studies to estimate the error variances associated with a number of physical and geophysical data sets. A key assumption in both methods is that the errors of the data sets are not correlated, although some studies have considered the effect of the partial correlation of representativeness errors in two or more of the data sets.

We compare the 3CH and 2CH methods using a simple model to simulate three and two data sets with various error correlations and biases. With this model, we know the exact error variances and covariances, which we use to assess the accuracy of the 3CH and 2CH estimates. We examine the sensitivity of the estimated error variances to the degree of error correlation between two of the data sets as well as the sample size. We find that the 3CH method is less sensitive to these factors than the 2CH method and hence is more accurate. We also find that biases in one of the data sets has a minimal effect on the 3CH method, but can produce large errors in the 2CH method.

1 Introduction

In atmospheric sciences, observations and models are often combined with the goal of providing accurate and complete representations of the current or future state of the atmosphere. Knowing the error characteristics of observations and models is important to understanding the degree to which atmospheric phenomena of interest are accurately described and analyzed. Estimating observational and modeling error characteristics is thus of inherent scientific interest. In addition, knowing the error characteristics is important for practical applications such as data assimilation and numerical weather prediction. In many modern data assimilation schemes, observations of a given type are weighted proportionally to the inverse of their error variance (e.g. Desroziers and Ivanov, 2001).

There are several somewhat similar methods for estimating the error variances associated with two or more data sets. The “three-cornered hat” (3CH) method and the closely related “triple collocation” (TC) method have been used in physics, oceanography, and other scientific disciplines to estimate the errors associated with three independent data sets. Braun et al. (2001) combined two independent data sets, Global Positioning System (GPS) slant water vapor (SWV) and water vapor ra-

diometer (WVR), to estimate the SWV and WVR errors. In analogy to the 3CH method, we refer to the Braun et al. (2001) method as the two-cornered hat (2CH) method. Kuo et al. (2004) and Chen et al. (2011) used the “apparent error method”, which is a variation of the 2CH method, to estimate the error of radio occultation (RO) observations using the known (or estimated) error variance of a forecast model.

5 The 3CH method was originally developed as the “N-cornered hat” method (Gray and Allan, 1974) for estimating error variances from N atomic clocks. Requiring three data sets at a minimum, the 3CH method produces estimates of the error variances of each of three data sets. Riley (2003), and references therein, provide a summary of the 3CH method. Variations and enhancements of the method have been applied to many diverse geophysical data sets. The 3CH method has been used to estimate the stability of GNSS clocks using the measured frequencies from multiple clocks (Ekstrom and Koppang, 2006; 10 Griggs et al., 2014, 2015; Luna et al., 2017). Valty et al. (2013) used the 3CH method to estimate the geophysical load deformation computed from GRACE satellites, GPS vertical displacement measurements, and global general circulation (GCM) models. O’Carroll et al. (2008) compared three systems to measure sea-surface temperatures: two different radiometers and in situ observations from buoys. They discuss the assumption of neglecting the error correlations among the three data sets and the effect of representativeness errors. Anthes and Rieckh (2018) used the 3CH method to estimate the error variances of three 15 observational (two radio occultation retrievals and radiosondes) and two model data sets using various combinations of the five data sets.

The major assumption in all of the above methods is that the errors of the three systems are uncorrelated. Correlations between any or all of the three measurement systems will reduce the accuracy of the error estimates. Other factors that can reduce the accuracy include widely different errors associated with the three systems or a small sample size. These factors can 20 lead to negative estimates of error variances, especially when the estimates are close to zero (Gray and Allan, 1974; Riley, 2003; Griggs et al., 2014).

Stoffelen (1998) developed a closely related method, termed the “triple collocation” (TC) method, to estimate both errors and linear calibration coefficients of surface winds using three data sets. Stoffelen (1998) discussed the correlation between part of the representativeness errors of two of the data sets and subtracted the variance common to the scale of these errors from 25 the estimated error variance of one of the data sets used in his pairwise estimate of error variances. This correction requires an independent estimate of the correlated part of the representativeness error. All variations of TC methods assume that, apart from the correlated part of the representativeness errors, the errors of the different observation systems are uncorrelated.

Variations of Stoffelen’s TC method have been widely used in the fields of oceanography and hydrometeorology (e.g. Su et al., 2014; Gruber et al., 2016). Roebeling et al. (2012) used the TC method to estimate the errors associated with 30 three ways of measuring precipitation: the Spinning Enhanced Visible and Infrared Imager (SEVERI), weather radars, and ground-based rain gauges.

In this paper we estimate the effect of neglecting the error covariances using two or three simulated data sets for which the true error variances and covariances are known. We develop a model to simulate the data sets with random and bias errors using a set of assumed True profiles. We then calculate the true error variance and covariance terms in the simulated data sets 35 and show the impact of neglecting these terms on the estimated error variances.

2 Error estimates using the 2CH and 3CH methods

We assume we have three data sets X, Y, and Z that are all measuring the same physical variable, e.g. specific humidity, q , at the same location and time.

The *error variance* of the data set X is defined as

$$5 \quad \text{VAR}_{\text{err}}(X) = \frac{1}{n} \sum (X - \text{True})^2 = \frac{1}{n} \sum X_{\text{err}}^2 \quad (1)$$

where True is the true (but unknown) value of X (as well as Y and Z), $X_{\text{err}} = (X - \text{True})$, and n is the number of samples. O’Carroll et al. (2008) provide an excellent discussion of the meaning of “True” in the context of the 3CH method.

The *error covariance* of the data sets X and Y is defined as

$$\text{COV}_{\text{err}}(X, Z) = \frac{1}{n} \sum (X - \text{True})(Y - \text{True}) \quad (2)$$

10 In general, the errors of X, Y, and Z may be correlated or not.

2.1 Three-cornered hat (3CH) method

In the 3CH method, the relationship between the error variances, the mean square (MS) differences of X and Y ($\text{MS}(X-Y)$), and their error covariances are given by Eqs. (7)–(9) of Anthes and Rieckh (2018):

$$\begin{aligned} \text{VAR}_{\text{err}}(X) = & \frac{1}{2} [\text{MS}(X - Y) + \text{MS}(X - Z) - \text{MS}(Y - Z)] \\ & + \text{COV}_{\text{err}}(X, Y) + \text{COV}_{\text{err}}(X, Z) - \text{COV}_{\text{err}}(Y, Z) \end{aligned} \quad (3)$$

15

$$\begin{aligned} \text{VAR}_{\text{err}}(Y) = & \frac{1}{2} [\text{MS}(X - Y) + \text{MS}(Y - Z) - \text{MS}(X - Z)] \\ & + \text{COV}_{\text{err}}(X, Y) + \text{COV}_{\text{err}}(Y, Z) - \text{COV}_{\text{err}}(X, Z) \end{aligned} \quad (4)$$

$$\begin{aligned} \text{VAR}_{\text{err}}(Z) = & \frac{1}{2} [\text{MS}(X - Z) + \text{MS}(Y - Z) - \text{MS}(X - Y)] \\ & + \text{COV}_{\text{err}}(X, Z) + \text{COV}_{\text{err}}(Y, Z) - \text{COV}_{\text{err}}(X, Y) \end{aligned} \quad (5)$$

We note that Eqs. (3)–(5) are identical to Eq. (1) in O’Carroll et al. (2008) in their application of the TC method to estimate the error variances of sea surface temperature using observations from two satellite systems and in-situ buoys.

The last three covariance terms in Eqs. (3)–(5) are unknown for real data sets, unless they are estimated independently, and are neglected when estimating the error variances of the real data sets X, Y and Z. This assumption is valid for no correlation between the errors of the data sets and a large sample size. The estimated error variances are therefore:

$$\text{VAR}_{\text{err}}(X)_{\text{est}} = \frac{1}{2} [\text{MS}(X - Y) + \text{MS}(X - Z) - \text{MS}(Y - Z)] \quad (3a)$$

$$25 \quad \text{VAR}_{\text{err}}(Y)_{\text{est}} = \frac{1}{2} [\text{MS}(X - Y) + \text{MS}(Y - Z) - \text{MS}(X - Z)] \quad (4a)$$

$$\text{VAR}_{\text{err}}(Z)_{\text{est}} = \frac{1}{2} [\text{MS}(X - Z) + \text{MS}(Y - Z) - \text{MS}(X - Y)] \quad (5a)$$

2.2 Two-cornered hat (2CH) method

The 2CH method uses only two data sets, X and Z. The derivation is presented in Appendix A. The 2CH method error variances for X and Z are given as

$$\begin{aligned} \text{VAR}_{\text{err}}(X) = & \text{MS}(X) - \frac{1}{4} [\text{MS}(X + Z) - \text{MS}(X - Z)] \\ & - 2\text{M}(\text{True}, X_{\text{err}}) + \text{COV}_{\text{err}}(X, Z) + \text{M}(\text{True}, X_{\text{err}} + Z_{\text{err}}) \end{aligned} \quad (6)$$

5 and

$$\begin{aligned} \text{VAR}_{\text{err}}(Z) = & \text{MS}(Z) - \frac{1}{4} [\text{MS}(X + Z) - \text{MS}(X - Z)] \\ & - 2\text{M}(\text{True}, Z_{\text{err}}) + \text{COV}_{\text{err}}(X, Z) + \text{M}(\text{True}, X_{\text{err}} + Z_{\text{err}}). \end{aligned} \quad (7)$$

where $\text{M}(X)$ is the mean value of X. The last three error terms in Eq. (6) and (7) are unknown for real data sets, unless they are estimated independently, and are neglected when estimating the error variances of the real data sets X and Z:

$$\text{VAR}_{\text{err}}(X)_{\text{est}} = \text{MS}(X) - \frac{1}{4} [\text{MS}(X + Z) - \text{MS}(X - Z)] \quad (6a)$$

$$10 \quad \text{VAR}_{\text{err}}(Z)_{\text{est}} = \text{MS}(Z) - \frac{1}{4} [\text{MS}(X + Z) - \text{MS}(X - Z)]. \quad (7a)$$

Equations (6a) and (7a) are equivalent to Eqs. (12) and (13) of Braun et al. (2001).

An alternative form of Eqs. (6a) and (7a) that is used in some studies (e.g. Stoffelen, 1998; Vogelzang et al., 2011) is

$$\text{VAR}_{\text{err}}(X)_{\text{est}} = \text{MS}(X) - \text{M}(XZ) \quad (6b)$$

$$\text{VAR}_{\text{err}}(Z)_{\text{est}} = \text{MS}(Z) - \text{M}(XZ). \quad (7b)$$

15 2.3 Comparison of neglected terms in 3CH and 2CH methods

In the 3CH method, the neglected error terms when computing $\text{VAR}_{\text{err}}(X)$ with Eq. (3) are

$$\text{COV}_{\text{err}}(X, Y) + \text{COV}_{\text{err}}(X, Z) - \text{COV}_{\text{err}}(Y, Z).$$

In the 2CH method, the neglected error terms when computing VAR_{err} with Eq. (6) are

$$- 2 \text{M}(\text{True}, X_{\text{err}}) + \text{COV}_{\text{err}}(X, Z) + \text{M}(\text{True}, X_{\text{err}} + Z_{\text{err}}).$$

20 We note that the neglected error terms in the 2CH method contain terms involving the product of True with errors, unlike in the 3CH method. Because True is typically an order of magnitude greater than the errors, these terms are likely much larger than the neglected terms involving only products of errors, as in the 3CH method. We also note that if the errors are random and uncorrelated, all of the error terms will be zero for an infinite sample size. However, for finite sample sizes, these terms will be non-zero even if these conditions are met.

25 2.4 Side note: apparent error method

We note that Eq. (A7) in Appendix A is the basis for the ‘‘apparent error’’ (AE) method in which X is an observed data set (X_{obs}) and Z is a forecast of the X data set (X_{fcst})

$$AE = X_{\text{obs}} - X_{\text{fcst}}$$

$$\text{VAR}_{\text{err}}(X_{\text{obs}}) = \text{MS}(X_{\text{obs}} - X_{\text{fcst}}) - \text{VAR}_{\text{err}}(X_{\text{fcst}}) + 2 \text{COV}_{\text{err}}(X_{\text{obs}}, X_{\text{fcst}})$$

The apparent error is equivalent to the Observation minus Background (O – B) statistic used in data assimilation studies. In the apparent error method, the correlation of errors between the observations and forecasts is assumed negligible and the error variance of the forecast is obtained from an independent estimate.

3 Generation of True data set and three simulated data sets with errors

We first generate a set of n vertical profiles of a variable, True, which we take as specific humidity from the ERA-Interim reanalysis (Dee et al., 2011), normalized by the mean specific humidity \bar{q} averaged over all samples. We next generate three data sets X, Y and Z that are approximations of True (True plus random errors), where the errors of X and Z are correlated to a degree that we can control. For simplicity, we assume the errors for Y are always uncorrelated with those of X and Z. This is analogous to a system of three observational systems in which the errors of two of them are correlated, but the errors of the third are not. In this section, only random errors are considered. The effect of bias errors is discussed in Sect. 4.4.2.

We then look at the magnitude of the error terms in the 2CH and 3CH methods with various assumed correlation coefficients between the errors in X and Z and compare the estimated error variances of X, Y and Z with their true error variances. Our tests will show the impact of the neglect of the error terms depending on the degree of error correlation between X and Z.

The assumed normalized random error model for X is given by

$$X_{\text{err}} = \text{random}[-1.7, 1.7] \cdot \text{STD} \quad (8)$$

$$\text{STD} = 0.1 + 0.00042 \cdot (1000 - p) \quad (9)$$

where $\text{random}[-1.7, 1.7]$ is a random number between -1.7 and 1.7 , and the standard deviation STD increases linearly with decreasing pressure p from a value of 0.1 (10 %) at 1000 hPa to a value of 0.436 (43.6 %) at 200 hPa. In the estimated error calculations below, the normalized X_{err} is expressed as a % error and the variance is expressed as %².

The error model is created based on error estimates of specific humidity from several studies (e.g. Kursinski et al., 1997; Collard and Healy, 2003; von Engel and Nedoluha, 2005; Wang et al., 2013). For example, Collard and Healy (2003) found that, for tropical conditions, the percentage errors for RO specific humidity varied from approximately 10 % near the surface to about 70 % near 300 hPa. Other studies show the errors varying from about 10 % near the surface to 100 % in the upper troposphere (about 200 hPa). In our error model, we specified the STD to roughly approximate the STD of RO or RS data at Minamidaitojima, Japan (Anthes and Rieckh, 2018; Rieckh et al., 2018). The assumed STD of normalized q (percent error) given by Eq. (9) is consistent with the above empirical error estimates. Thus the error model is a reasonable one in terms of its magnitude and increase with height. Since it is intended to show the sensitivity of the 3CH and 2CH methods to varying degrees of correlation between two of the data sets used in the comparison, it is not necessary that the error model be a close replication of any particular observing system, just that the magnitude of the assumed errors and their vertical distribution be reasonable.

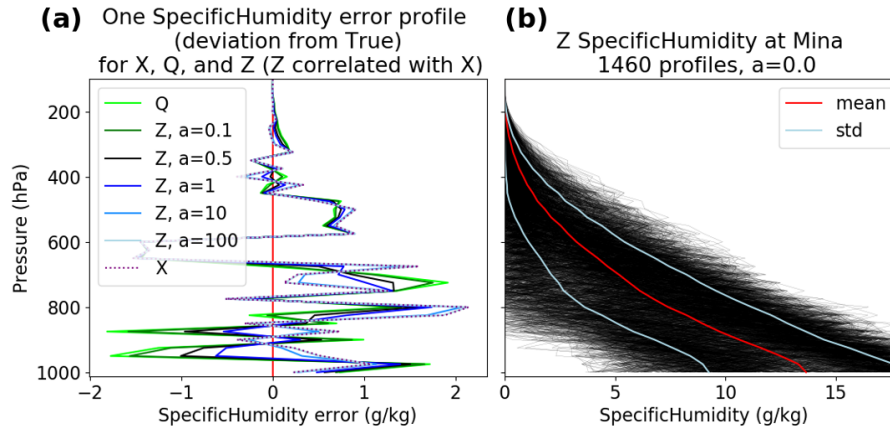


Figure 1. (a) One set of error profiles with the unnormalized X_{err} (dotted line), Q_{err} (solid lime green line) and Z_{err} (various solid lines for different values of correlation parameter a). Q_{err} is uncorrelated with X_{err} . For $a = 0$, $Z_{\text{err}} = Q_{\text{err}}$ and Z_{err} and X_{err} are uncorrelated. As a increases, Z_{err} is increasingly correlated with X_{err} and looks less like Q_{err} and more like X_{err} . For very large a ($a = 100$), Z_{err} (light blue solid line) is almost equal to X_{err} (dotted line). (b) 1460 profiles of the unnormalized data set Z with zero correlation with X ($a = 0$).

3.1 Calculation of correlated errors

In the calculation of the correlated errors, we first generate the random error profiles X_{err} , Y_{err} , and Q_{err} . All of these error profiles are uncorrelated. In general all three error profiles X_{err} , Y_{err} , and Q_{err} may have different standard deviations, but for these tests we assume all standard deviations vary according to Eq. (9) for simplicity. We now generate the error profile Z_{err} as a linear combination of X_{err} and Q_{err} :

$$Z_{\text{err}} = \frac{a \cdot X_{\text{err}} + Q_{\text{err}}}{1 + a} \quad (10)$$

where a is a specified constant parameter that determines the degree of correlation between Z_{err} and X_{err} . If $a = 0$, $Z_{\text{err}} = Q_{\text{err}}$ and the errors of X , Y and Z are all uncorrelated. If a is not equal 0, the errors of Z are correlated with the errors of X . Figure 1a shows one set of simulated error profiles for the unnormalized X , Q , and several Z for different values of a . The transition of Z_{err} from Q_{err} to X_{err} can be seen easily between 700 and 800 hPa. Q_{err} (bright green line) is positive (around 1 g kg^{-1}) and Z_{err} for $a = 0$ is identical to that. For $a = 0.1$, Z_{err} has a slightly smaller positive value, and Z_{err} becomes negative as a increases, becoming practically identical with X_{err} (dotted line) for $a = 100$.

Figure 1b shows the mean and standard deviation for the unnormalized Z specific humidity profiles for $a = 0$. Since the Z_{err} are created by combining the two random errors Q_{err} and X_{err} , the Z_{err} are overall closer to zero. This will result in a smaller standard deviation of Z if $0 < a < \infty$ (especially for values of a close to 1), and will also decrease the true error variance of Z .

3.2 Relationship of correlation, error variance, and error covariance terms

The correlation coefficient r between the X_{err} and Z_{err} is given by

$$r = \frac{1}{n} \sum \frac{(X_{\text{err}} - \bar{X}_{\text{err}})(Z_{\text{err}} - \bar{Z}_{\text{err}})}{\sigma_{X_{\text{err}}} \sigma_{Z_{\text{err}}}} \quad (11)$$

where \bar{X}_{err} and \bar{Z}_{err} are the mean values of X_{err} and Z_{err} respectively (zero in our error model) and $\sigma_{X_{\text{err}}}$ and $\sigma_{Z_{\text{err}}}$ are the

5 standard deviations of X_{err} and Z_{err} given by

$$\sigma_{X_{\text{err}}} = \sqrt{\frac{1}{n} \sum X_{\text{err}}^2} \equiv (\text{VAR}_{\text{err}}(X))^{1/2} \text{ using Eq. (1)}$$

$$\sigma_{Z_{\text{err}}} = \sqrt{\frac{1}{n} \sum Z_{\text{err}}^2} \equiv (\text{VAR}_{\text{err}}(Z))^{1/2} \text{ using Eq. (1)}$$

The relationship between the correlation coefficient and covariance between X_{err} and Z_{err} is therefore

10

$$\text{COV}(X_{\text{err}}, Z_{\text{err}}) = r \sigma_{X_{\text{err}}} \sigma_{Z_{\text{err}}} \equiv \text{COV}_{\text{err}}(X, Z) \text{ using Eq. (2).}$$

It can be shown that for this particular error model

$$r = \frac{a}{(1 + a^2)^{1/2}} \quad (12)$$

$$15 \quad \text{VAR}_{\text{err}}(Z) = \frac{(1 + a^2)}{(1 + a)^2} \text{VAR}_{\text{err}}(X) \quad (13)$$

$$\text{COV}_{\text{err}}(X, Z) = \frac{a}{(1 + a)} \text{VAR}_{\text{err}}(X) \quad (14)$$

The correlation between X and Z errors can be varied according to Eq. (12) by varying the parameter a , as shown in Table 1. Note that $\text{VAR}_{\text{err}}(Z) \leq \text{VAR}_{\text{err}}(X)$ and that the maximum difference between $\text{VAR}_{\text{err}}(X)$ and $\text{VAR}_{\text{err}}(Z)$ occurs for $a = 1$ when $\text{VAR}_{\text{err}}(Z) = 0.5 \text{VAR}_{\text{err}}(X)$ ($\sigma_{Z_{\text{err}}} = 0.707 \sigma_{X_{\text{err}}}$).

20 3.3 Summary of generation of True data set and simulated data sets with random and systematic errors

– We use 2007 ERA-Interim specific humidity q profiles for a location near Minamidaitojima (hereafter Mina), Japan, which is located on Okinawa at 25.6°N 131.5°W. There are four model data profiles per day or $n = 1460$ profiles.

– Assume each vertical profile of q has no error, and normalize the q at each level by the sample mean (\bar{q}) at that level. This is the True data set.

25 – Generate three different and independent random error profiles X_{err} , Y_{err} and Q_{err} from Eqs. (8) and (9).

– Generate Z_{err} for various specified values of a to control correlation using Eq. (10).

– Add X_{err} , Y_{err} and Z_{err} to True to obtain X, Y and Z, the 1460 simulated normalized profiles of q .

– Compute the normalized estimated error variance profiles of X, Y and Z for the 3CH and 2CH methods according to Eqs. (3a)–(7a) (which have neglected all COV terms) and compare with the true error variances, which can be computed

Table 1. Relationship between normalized error variances and standard deviations of data sets X and Z for different values of a .

a	r	$\sigma_{Z_{\text{err}}}/\sigma_{X_{\text{err}}}$	$\text{VAR}_{\text{err}}(Z) (\% ^2)$	$\text{COV}_{\text{err}}(X, Z) (\% ^2)$
0.0	0.0	1.0	1.00 $\text{VAR}_{\text{err}}(X)$	0.0
0.1	0.0995	0.9136	0.84 $\text{VAR}_{\text{err}}(X)$	0.0909 $\text{VAR}_{\text{err}}(X)$
0.3	0.287	0.803	0.65 $\text{VAR}_{\text{err}}(X)$	0.230 $\text{VAR}_{\text{err}}(X)$
0.5	0.447	0.745	0.55 $\text{VAR}_{\text{err}}(X)$	0.333 $\text{VAR}_{\text{err}}(X)$
1.0	0.707	0.707	0.50 $\text{VAR}_{\text{err}}(X)$	0.500 $\text{VAR}_{\text{err}}(X)$
2.0	0.894	0.745	0.55 $\text{VAR}_{\text{err}}(X)$	0.666 $\text{VAR}_{\text{err}}(X)$
10.0	0.995	0.913	0.83 $\text{VAR}_{\text{err}}(X)$	0.908 $\text{VAR}_{\text{err}}(X)$
100.0	0.99995	0.9901	0.98 $\text{VAR}_{\text{err}}(X)$	0.990 $\text{VAR}_{\text{err}}(X)$
∞	1.0	1.0	1.00 $\text{VAR}_{\text{err}}(X)$	1.0 $\text{VAR}_{\text{err}}(X)$

exactly from the full Eqs. (3)–(7) including the known values of the covariance terms. A value of $a = 0$ should give the most accurate estimation of error variances because all covariance terms will be close to zero (they won't be exactly zero because the sample size n is finite).

4 Effect of error correlations on estimated error variances

5 We now derive expressions for the estimated values of the error variances for X, Y and Z for this error model and show how the correlations between X_{err} and Z_{err} affect the approximate values using the 3CH and 2CH methods. This will give some insight into how correlations between actual observed data sets will affect estimates of their error variances and standard deviations. To make results more readily comparable to previous studies, instead of showing the error variance, we show the square root of the error variance, or the error standard deviation, in most figures.

10 4.1 Effect of error correlations on 3CH method

In the 3CH method, three covariance terms are neglected. These terms are zero for an infinite sample size for uncorrelated errors between the data sets. Correlation between the errors of two data sets will lead to a non-zero covariance term, which becomes larger for larger correlations. The error covariances $\text{COV}_{\text{err}}(X, Z)$, $\text{COV}_{\text{err}}(X, Y)$ and $\text{COV}_{\text{err}}(Y, Z)$ are shown in Fig. 2 for $a = 0$ and 0.5. Note that all error covariances oscillate around zero (and are zero for an infinitely large sample size) for $a = 0$ (Fig. 2a). For $a = 0.5$, the $\text{COV}_{\text{err}}(X, Z)$ term increases with decreasing pressure, reaching a magnitude of about 800 $\% ^2$ at 100 hPa (Fig. 2b).

For our model (error correlation of X and Z) and an infinite sample size, $\text{COV}_{\text{err}}(X, Z)$ is the only non-zero neglected term in Eq. (3a). Therefore Eq. (3a) can also be expressed as

$$\text{VAR}_{\text{err}}(X)_{\text{est}} = \text{VAR}_{\text{err}}(X) - \text{COV}_{\text{err}}(X, Z) \quad (2b)$$

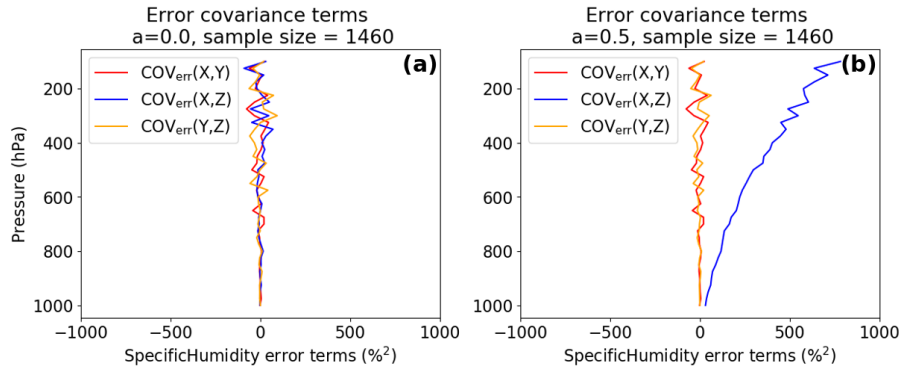


Figure 2. Vertical profiles of normalized error covariances (X, Y), (Y, Z) and (X, Z) for: (a) $a = 0$ and (b) $a = 0.5$.

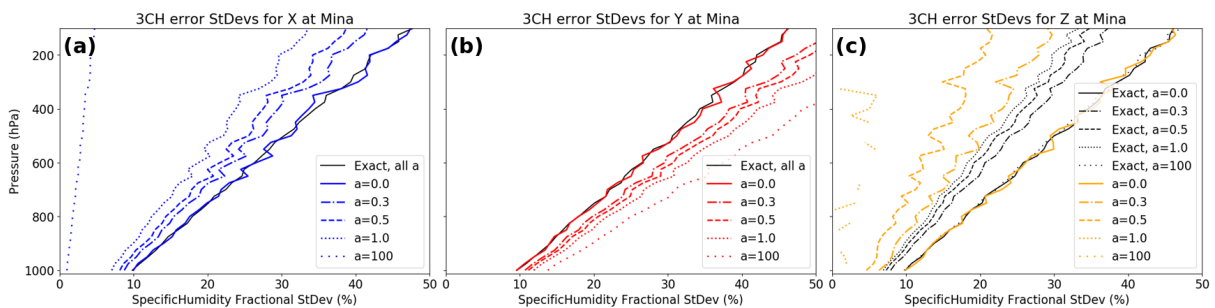


Figure 3. (a) Estimated standard deviation of X_{err} for values of $a = 0, 0.3, 0.5, 1.0$ and 100 computed from Eq. (3a)–(5a). Exact STD computed from data set X (solid black profile). (b) Same as (a) except for estimated STD of Y_{err} . (c) Same as (a) except for estimated STD of Z_{err} . Note that for different values of a , the exact STD of X_{err} and Y_{err} are always the same. The exact STD of Z_{err} decreases as a increases for $0 < a < 1.0$. For $a > 1.0$, the exact STD of Z_{err} increases as a increases, becoming equal to the STD of X_{err} for $a = \infty$ due to the way our error model is defined (see also Table 1). For $a = 100$ the correlation between X and Z errors is 0.99995 (Table 1; black dotted line for $a = 100$ almost identical to black solid line for $a = 0$).

Using Eq. (14) for this error model yields

$$\text{VAR}_{\text{err}}(X)_{\text{est}} = [1/(1+a)]\text{VAR}_{\text{err}}(X). \quad (2c)$$

Hence for $a > 0$ the estimated error variance of X is always less than the true value, as seen in Fig. 3a.

We next consider the effect of the X and Z error correlation on the estimate for Y error variance. For our error model, Eq. (4a) can be expressed as

$$\text{VAR}_{\text{err}}(Y)_{\text{est}} = \text{VAR}_{\text{err}}(Y) + \text{COV}_{\text{err}}(X, Z). \quad (3b)$$

Substituting for the COV term from Eq. (14) and noting that, for our error model, $\text{VAR}_{\text{err}}(X) = \text{VAR}_{\text{err}}(Y)$ we obtain

$$\text{VAR}_{\text{err}}(Y)_{\text{est}} = [(1 + 2a)/(1 + a)]\text{VAR}_{\text{err}}(Y) \quad (3c)$$

Thus the estimated error variance for Y is always greater than the true value for $a > 0$, which is seen in Fig. 3b.

5 Lastly, we consider the effect of the X and Z correlation on the estimate for the Z error variance. Eq. (5a) can be expressed as

$$\text{VAR}_{\text{err}}(Z)_{\text{est}} = \text{VAR}_{\text{err}}(Z) - \text{COV}_{\text{err}}(X, Z). \quad (4b)$$

Substituting for the COV term from Eq. (14) and using Eq. (13) we obtain

$$\text{VAR}_{\text{err}}(Z)_{\text{est}} = [(1 - a)/(1 + a^2)]\text{VAR}_{\text{err}}(Z) \quad (4c)$$

so that the estimated error variance for Z is less than the true value for $a > 0$, which is illustrated in Fig. 3c. Finally, for $a > 1$,
 10 Eq. (4c) shows that the estimated error variance of Z is negative and the STD is undefined. For $a = 1.0$, the estimated error variance of Z is zero for an infinite data set, but oscillates around zero because of our finite data set. Thus the estimated STD of Z_{err} is undefined at some levels (Fig. 3c).

4.2 Summary of error correlations on 3CH method

For the 3CH method, correlation between the data sets X and Z has the following affect on their computed error variances
 15 (when covariance terms are neglected):

$$\text{VAR}_{\text{err}}(X)_{\text{est}} < \text{VAR}_{\text{err}}(X)_{\text{true}}$$

$$\text{VAR}_{\text{err}}(Y)_{\text{est}} > \text{VAR}_{\text{err}}(Y)_{\text{true}}$$

$$\text{VAR}_{\text{err}}(Z)_{\text{est}} < \text{VAR}_{\text{err}}(Z)_{\text{true}}$$

Figure 4 shows the ratios of the approximate error variances and standard deviations to the true values for a ranging from
 20 0 to 1 for the 3CH method. As the correlation parameter a increases from 0, the differences between the estimated and true error variances increase. For a modest value of $a = 0.2$ (correlation coefficient between X and Z errors of 0.196), the errors in the STD estimates are -9% for X, $+8\%$ for Y and -12% for Z. As the correlation between the X and Z error reach 0.5, the percentage errors for the X, Y and Z estimates reach -18% , $+14.5\%$ and -37% respectively. To the extent that this error model gives an idea of the effect of the correlation between the errors of two of the three data sets, estimates of error standard
 25 deviations using a large sample of real data should be accurate to within approximately 10% for correlation coefficients between data errors of 0.2 or below, and within 25% for correlation coefficients of around 0.3. The effect of the correlation between Z and X errors on the estimated error variance is greatest on the estimated Z error variance.

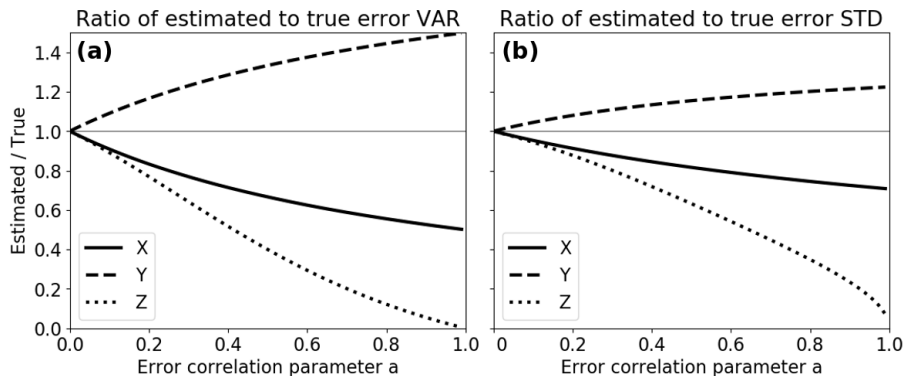


Figure 4. Ratio of estimated (a) error variances to true variances and (b) estimated STD to true STD for the 3CH method for values of error correlation parameter a ranging from 0 to 1.0.

4.3 Effect of error correlations on 2CH method

We next examine how error correlations in our error model affect the 2CH method. To estimate the error variance of X using Eq. (6a), we calculate examples of the error terms for $a = 0$ and $a = 0.5$. The $\text{COV}_{\text{err}}(X, Z)$ term was already shown in Fig. 2, and is the same in the 2CH method as in the 3CH method. Figures 5 and 6 show profiles of the other two terms for an error correlation between X and Z of $a = 0$ and 0.5. In our error model X_{err} and Z_{err} are uncorrelated with True, so the non-zero values in Figs. 5–6 are a result of the finite data set (1460 in this example). The $\text{COV}_{\text{err}}(X, Z)$ (Fig. 2) increases as a increases, reaching a maximum value in the upper troposphere of about $800\% ^2$ for $a = 0.5$. The terms involving True and the errors in X, Y and Z in Figs. 5 and 6 do not change in magnitude with an increasing value of a , but they increase in amplitude with height and are significantly large ($\sim 300\% ^2$) compared to the $\text{COV}_{\text{err}}(X, Z)$. These results indicate that a large sample size is especially important in the 2CH method; even with a sample size of 1460 the random errors caused by the neglect of the covariance terms involving True and the errors in X and Z can be significant.

Figure 7 shows the exact and estimated error STD of X , Y , and Z for various combinations of the data sets and values of a . The estimated error STD for X , Y , and Z vary around the exact solutions (black lines) for all values of a if data sets with uncorrelated errors are combined: (a) $\text{STD}_{\text{err}}(X)$ computed with Y , (b) $\text{STD}_{\text{err}}(Y)$ computed with X , and (c) $\text{STD}_{\text{err}}(Z)$ computed with Y , and (e) $\text{STD}_{\text{err}}(Y)$ using Z . Note in (c) the exact $\text{STD}_{\text{err}}(Z)$ decreases with a increasing from 0 to 1, as described previously. Figs. 7(d) and (f) show how correlated errors between the data sets affect the estimated error variances. Both the estimated $\text{STD}_{\text{err}}(X)$ and $\text{STD}_{\text{err}}(Z)$ become too small when the data sets X and Z are combined and the value of a is increased. The exact solutions for all values of a in (f) are in black.

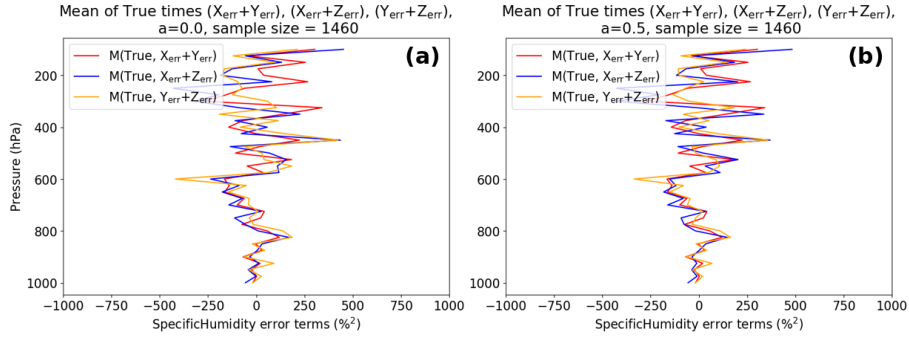


Figure 5. Terms involving products of True and $(X_{\text{err}} + Z_{\text{err}})$, $(X_{\text{err}} + Y_{\text{err}})$, and $(Y_{\text{err}} + Z_{\text{err}})$ for (a) $a = 0$ and (b) $a = 0.5$. Note that the magnitudes of True and $(X_{\text{err}} + Y_{\text{err}})$ and True and $(Y_{\text{err}} + Z_{\text{err}})$ do not depend on the correlation between X_{err} and Z_{err} . All error terms are normalized.

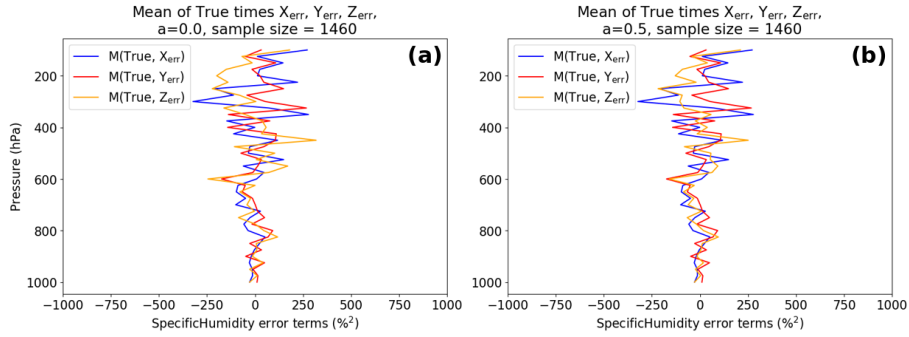


Figure 6. Mean of products of True and X_{err} , Y_{err} , and Z_{err} for (a) $a = 0$ and (b) $a = 0.5$. All error terms are normalized.

4.4 Comparison of 3CH and 2CH methods using the error model

4.4.1 Effect of random errors

Figure 8 compares the normalized error estimates from the 3CH and 2CH methods for $a = 0.5$. In Fig. 8a (3CH) the solid lines denote exact error STD of X, Y and Z. The exact error STD are the same for X and Y, and are smaller for Z as discussed earlier.

- 5 The estimated error STD (dashed lines) are less than the exact values for X and Z and greater than the exact values for Y, also as discussed earlier. In Fig. 8b (2CH), solid lines denote a combination of data sets with uncorrelated errors (where error terms are neglected, but are non-zero due to a finite sample size), while dashed lines indicate combinations of data sets with correlated errors and neglected error terms. We see that for the 3CH method and 2CH method all estimates are similar, with the exception of $\text{STD}_{\text{err}}(Y)$, which is affected in the 3CH method by correlation of X_{err} and Z_{err} . However, the profiles of the

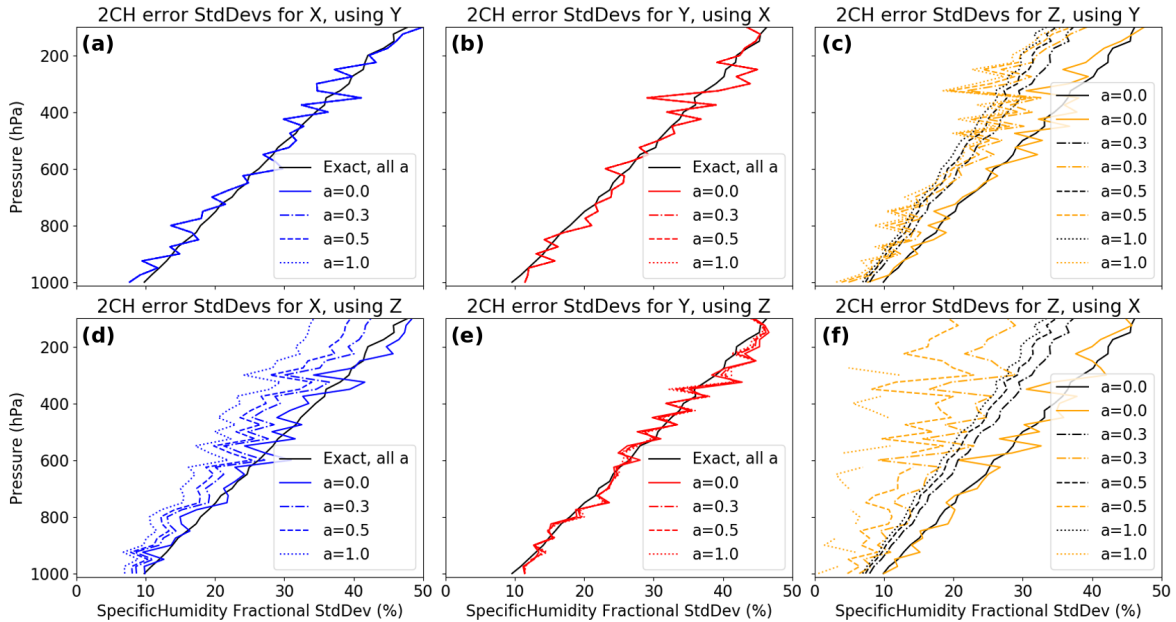


Figure 7. Two 2CH results each for the normalized error STD for X (a and d), Y (b and e) and Z (c and f), depending on the second data set. Profiles corresponding to several values of correlation parameter a are included. The solid black profile is the exact error STD profile for X and Y for all values of a , and for Z when $a = 0$.

2CH estimates show considerably more noise than those of the 3CH estimates, which is a consequence of the larger magnitude of the neglected error terms in the 2CH method (see Sects. 2.3 and 4 above).

We next consider the effect of the sample size on the error estimates from the 3CH and 2CH methods. We repeat the calculations from both methods by using a subset of the 1460 samples used in the above calculations. We created the subset by selecting every tenth sample from the complete set, giving a sample size of 146.

Figure 9 shows the same estimates as those in Fig. 8, except for the much smaller sample size of 146. For the smaller sample size, the noise increases for both methods. However, the effect on the 3CH method is less than on the 2CH method, and the differences in the estimates are still clearly visible in the 3CH method. For some of our comparison data sets using real data (Anthes and Rieckh, 2018), the sample size n is less than 100 in the lower and upper troposphere; hence the noise due to small sampling size is likely to be significant in the estimates for these regions.

4.4.2 Effect of bias errors

To investigate the effect of both random and systematic errors, we add a known bias ϵ to data set Z.

For the 3CH method, Eq. (3a) becomes

$$\text{VAR}_{\text{err}}(X)_{\text{est}} = \frac{1}{2}[\text{MS}(X - Y) + \text{MS}(X - (Z + \epsilon)) - \text{MS}(Y - (Z + \epsilon))] \quad (15)$$

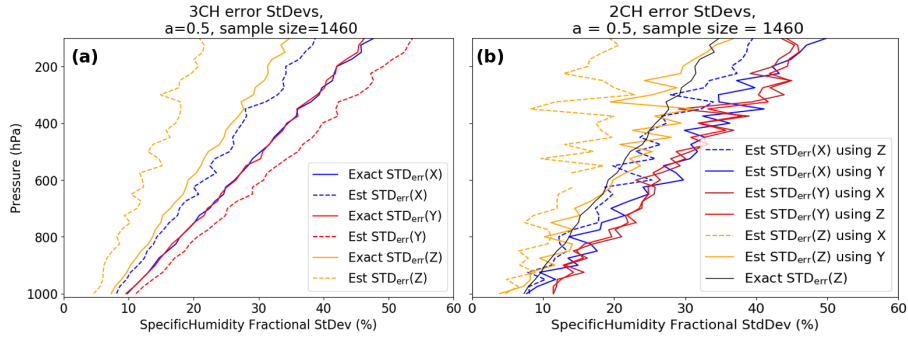


Figure 8. Estimated and exact normalized error standard deviations for 3CH method (a) and 2CH method (b) for a correlation of Z and X errors of 0.45 ($a = 0.5$). (a) Exact STD errors for X, Y and Z given by blue, red and orange solid lines respectively. Estimated error STD error given by dashed lines of same color. (b) Exact error STD of Z given by solid black line. Estimated error STD of X using Z and Y given by blue lines, estimated error STD of Y using X and Z given by red lines, and estimated error STD of Z using X and Y given by orange lines. For all colored lines, error terms are neglected. Solid lines indicate estimates from combinations of data sets with uncorrelated errors, dashed lines indicate estimates from combinations of data sets with correlated errors and hence larger error terms.

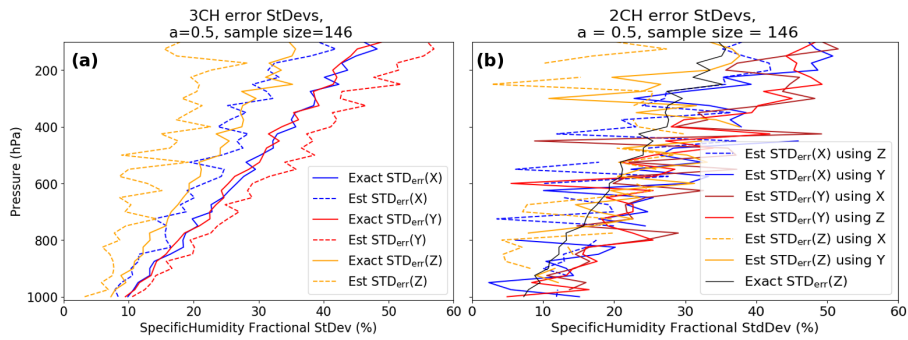


Figure 9. Same as Fig. 8 except for a smaller sample size of 146. All profiles become much noisier, with the 2CH method showing significantly more noise than the 3CH method.

which may be expanded to

$$\text{VAR}_{\text{err}}(X)_{\text{est}} = 1/2[\text{MS}(X - Y) + \text{MS}(X - Z) - \text{MS}(Y - Z)] + \epsilon M[(Y_{\text{err}} - X_{\text{err}})] \quad (16)$$

which is equal to Eq. (3a) plus the bias term. For random errors and a large sample size the means of X_{err} and Y_{err} will be very small and the difference of the mean errors will also be small. Thus the bias term will tend toward zero as the sample size increases and the effect of a bias error in Z is minimal in the 3CH method.

This is not the case in the 2CH method, as shown below. Equation (6a) becomes

$$\text{VAR}_{\text{err}}(X)_{\text{est}} = \text{MS}(X) - 1/4 [\text{MS}(X + (Z+\epsilon)) - \text{MS}(X - (Z+\epsilon))] \quad (17)$$

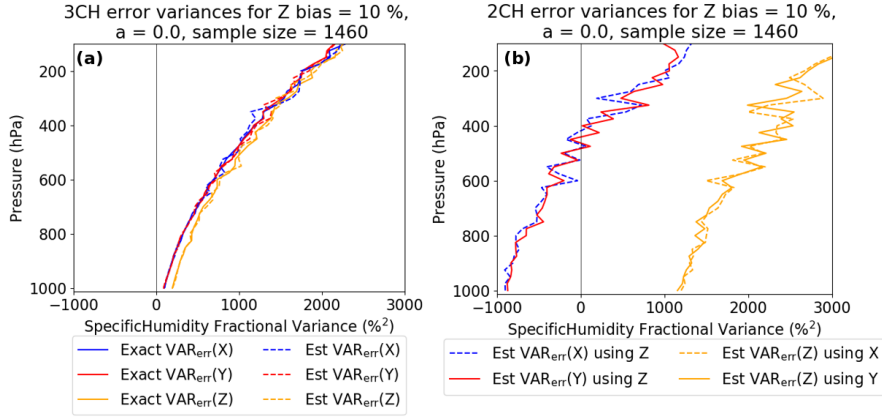


Figure 10. Effect of adding a constant bias of 10 % to Z for the 3CH (a) and 2CH (b) methods, for no correlation between X and Z errors (i.e. $a = 0$). The 3CH method yields reasonable estimates for all variables, while the estimated error variances from the 2CH method are erroneously large for Z (orange) and erroneously low X and Y (blue and red).

which can be expanded to

$$\text{VAR}_{\text{err}}(X)_{\text{est}} = \text{MS}(X) - \frac{1}{4} [\text{MS}(X + Z) - \text{MS}(X - Z)] - \epsilon M(X) \quad (18)$$

which is equal to Eq. (6a) plus a bias term.

As noted above, the bias term in the 3CH method can be close to zero and therefore not affect the computed $\text{VAR}_{\text{err}}(X)$ significantly. The bias term of the 2CH method will stabilize with higher sample sizes around the product of the bias (ϵ) and the $M(X)$ and will significantly influence the estimated error variance. A positive bias in the data set Z will cause a negative error in $\text{VAR}_{\text{err}}(X)$, and a negative bias in the data set Z will cause a positive error in $\text{VAR}_{\text{err}}(X)$.

For the simulated data set, Eq. (10) becomes

$$Z_{\text{err}} = \frac{a \cdot X_{\text{err}} + Q_{\text{err}}}{1 + a} + \epsilon, \quad (19)$$

10 while X_{err} and Y_{err} stay the same.

Figure 10 shows the effect of adding a constant bias of 10 % to Z for the 3CH and 2CH methods for no correlation of random errors ($a = 0$). For the 3CH method (Figure 10a), results still look reasonable, and the estimated and exact solutions overlap well. For the 2CH method (Figure 10b), a bias of 10 % strongly impacts the estimated error variances. For Z, they are much too high, and for X and Y they are much too low. Recalling that the variables X, Y, Z and ϵ are all normalized by the sample mean \bar{q} , $M(X)$ in Eq. (18) is approximately 100 %, so the term $\epsilon M(X)$ is approximately $100 \epsilon \%^2$. For $\epsilon = 10\%$, this term is $1000 \%^2$, which is the offset we see for X, Y, and Z in Fig. 10b.

4.4.3 General expression for effect of biases in all three data sets

More generally, we can derive expressions for the effect of biases of all three data sets with respect to True as follows (Sergey Sokolovskiy, 2018, personal communication): Let

$$X = \text{True} + X_{\text{err}} + \epsilon_X \quad (20)$$

$$5 \quad Y = \text{True} + Y_{\text{err}} + \epsilon_Y \quad (21)$$

$$Z = \text{True} + Z_{\text{err}} + \epsilon_Z \quad (22)$$

where ϵ_X , ϵ_Y , and ϵ_Z are biases of X, Y, and Z, respectively. Substituting these expressions into Eq. (3a) for the 3CH method and Eq. (6a) for the 2CH method, we find that the difference Δ between the error estimates for X with biases and those without biases is

$$10 \quad \Delta_{2\text{CH}} = (M(\text{True}) + \epsilon_X)(\epsilon_X - \epsilon_Y) \quad (23)$$

$$\Delta_{3\text{CH}} = \epsilon_X \cdot (\epsilon_Y - \epsilon_Z) + \epsilon_Y \epsilon_Z \quad (24)$$

The first term of Eq. (23) is a first order term while all the other terms are second order; thus in general biases will have a larger effect in the 2CH method compared to the 3CH method. We note that this expression is valid only for an infinite data set.

5 Estimates of error variances using 3CH and 2CH methods and real observations

15 Anthes and Rieckh (2018) showed a large number of error variance estimates using real data and the 3CH method at four radiosonde (RS) locations in the Pacific Ocean region. Here we show a few examples of how the 2CH method compares with these 3CH estimates.

We use co-located data of radio occultation (RO), RS, and ERA-Interim (ERA) at Minamidaitojima (Mina), which is located on Okinawa at 25.6°N 131.5°W, and is one of the four RS stations studied by Anthes and Rieckh (2018) and Rieckh et al. 20 (2018). We use the RO-Direct method for computing RO specific humidity (uses NCEP Global Forecast System temperature to compute specific humidity q from observed RO refractivity). Details about the co-location criteria and specific humidity retrieval are described by Rieckh et al. (2018).

To compute error variances using the 2CH method, Eq. (6a) is applied for various combinations of the four data sets. Data pairs at each level are only used if data are available for all four data sets. All data sets are interpolated to a common 25 hPa 25 grid. Figure 11a shows the number of co-located profiles per pressure level. Figure 11b shows the normalized RS specific humidity values for these profiles.

The two model and the RO data sets are representative of similar horizontal scales (~ 100 km), while the radiosonde data are in-situ point measurements and therefore represent a much smaller horizontal scale. However, many studies (e.g. Ho et al., 2010a, b; Kuo et al., 2004; Chen et al., 2011) have used radiosonde data as correlative data for verifying models, RO, and other 30 data sets without applying corrections for representativeness errors. These results indicate that the different representative

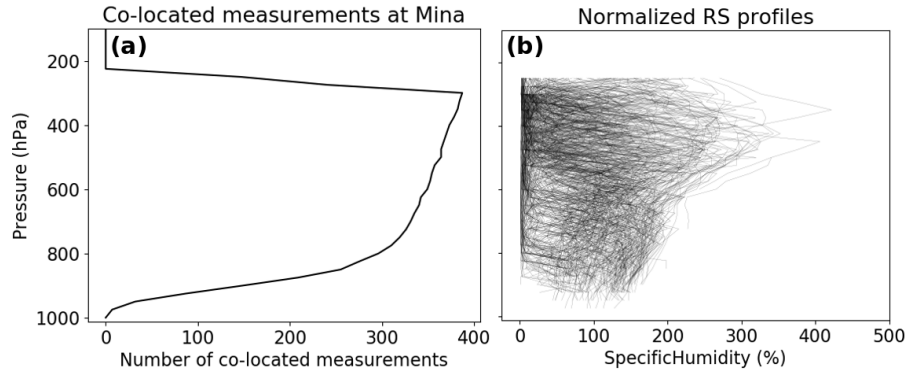


Figure 11. (a) Number of co-located measurements (data pairs) per pressure level for RO, RS, and ERA. (b) Normalized q values for radiosondes (RS) at Mina, 2007. The normalized q values are computed as $100 \cdot q / \bar{q}$ where \bar{q} is the annual mean value of q for 2007. Profiles cut off at 250 hPa because RS data are not reported at higher levels. At the bottom, co-located profiles thin out since RO penetration depth varies and only very few profiles are available at the lowest levels.

scales are not a significant source of error in the comparisons (unlike spatial and temporal sampling errors resulting from the time and spatial differences between the data sets, which we correct for). However, any representativeness errors are included in the error estimates using either the 2CH or 3CH method.

All four data sets have some degree of unknown bias for certain locations, altitudes, or atmospheric conditions; none of them represent the ultimate “truth” and there is no standard atmospheric data set for calibration. However, they have all been compared to other models or observations to one degree or another. We investigated the effect of biases in the related paper Anthes and Rieckh (2018) by calibrating the data sets to the ERA-Interim data set using the scaling coefficients as given by Stoffelen (1998) and Vogelzang et al. (2011). The results using the calibrated data sets were very similar to those using the uncalibrated data sets, confirming that the 3CH method is insensitive to small biases.

We use our results from the 3CH method for real data (Anthes and Rieckh, 2018) to evaluate the results of the 2CH method. Figure 12a shows the 3CH estimated error variances for specific humidity for ERA, RS and RO using three independent equations (Anthes and Rieckh, 2018). The mean value of the estimates is given by the solid line and the STD of the estimates about the mean by the shading. The 3CH estimates are considered reasonably accurate for the reasons given in Anthes and Rieckh (2018), namely that the magnitude and shape of the estimates for refractivity agree with other independent refractivity error estimates (so we assume that the method works just as well for humidity as for refractivity), and that the results are consistent for the four different RS stations studied.

The other panels in Fig. 12 show the 2CH estimates of the error variance for ERA (b), RO (c) and RS (d) using various pairs of observations. We consider the 2CH estimates unrealistic for these data sets. The magnitudes reach values that are negative or up to five times the magnitudes of the 3CH method, which is considered unrealistically large. The profiles of the estimates of error variances of ERA, RS and RO are also quite different depending on the pairs of observations used, unlike the 3CH

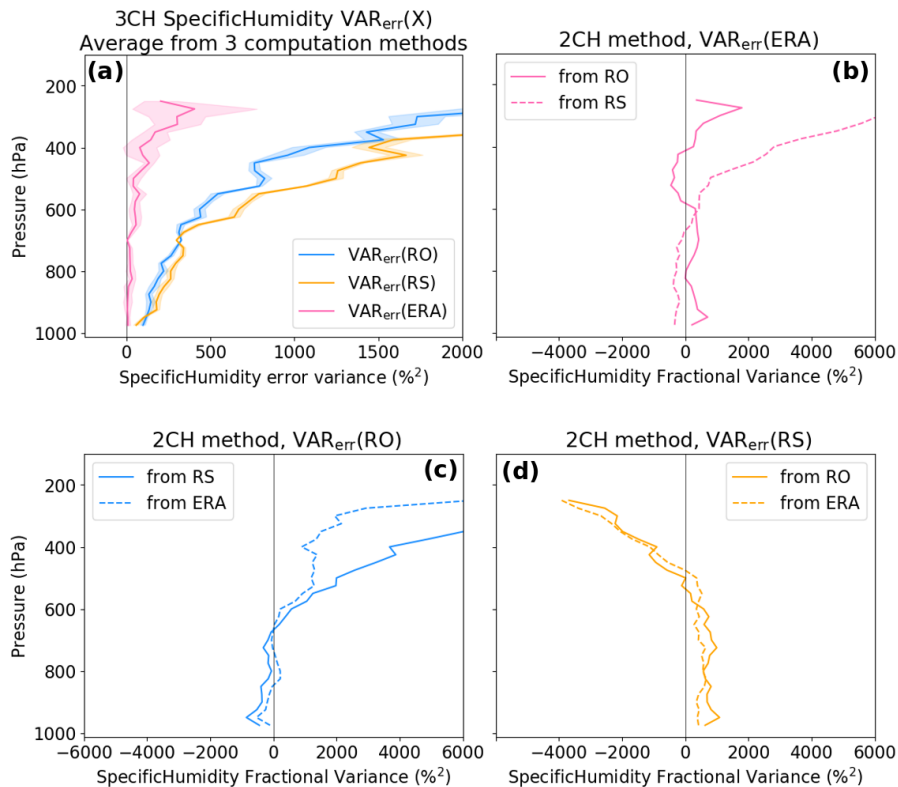


Figure 12. Estimated error variances for specific humidity: (a) results from the 3CH method for ERA (purple), RO (blue), and RS (orange). Other three panels: 2CH method estimates for ERA (b), RO (c) and RS (d).

method is which all combinations of observations give similar profiles. Similar results were obtained for 2CH estimates of refractivity (not shown).

Thus we find that the 2CH method produces estimates of the error variances for specific humidity that are quite different from those of the 3CH method. We suspected that the cause for the different behavior using real data might lie in the different treatment of bias errors in the 2CH and 3CH method. To investigate this hypothesis, we considered the effect of an empirically based bias in the simulated data.

5.1 Simulating the observed real data bias in the 2CH method

As shown in Sect. 4.4.2, even small bias errors in one of the data sets can cause large errors in the 2CH method. To see if a bias in our real data could explain the very different estimates of the error variances shown in Figs. 12b–12d for the 2CH method, we set up empirically based bias profiles in the simulated data. These match approximately the observed differences of RS and RO from ERA as found by Rieckh et al. (2018) in the real data sets (supplement, Figure S5 panel 4 for RS; Figure S6 panel 1 for RO). For the tests we consider ERA the truth. We computed the specific humidity annual mean biases of RO and RS for

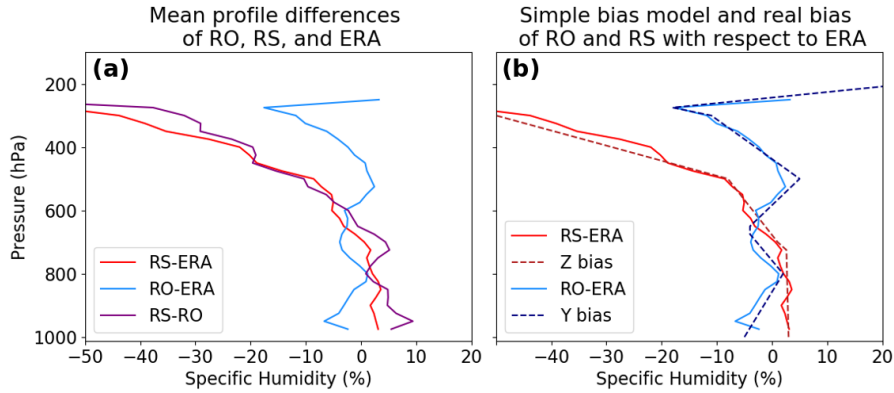


Figure 13. (a) Annual mean normalized profiles of RS – ERA, RO – ERA, and RS – RO. (b) same for RS – ERA and RO – ERA only (solid lines), and their respective empirical bias profiles (dashed lines) based on the mean profiles.

each level as $100[\text{Mean}(\text{RO}) - \text{Mean}(\text{ERA})]/\text{Mean}(\text{ERA})$ and $100[\text{Mean}(\text{RS}) - \text{Mean}(\text{ERA})]/\text{Mean}(\text{ERA})$, respectively. We used these results to create a simple additive bias for both Y and Z. The biases are depicted in Fig. 13 (dashed lines), along with the real RS and RO annual mean biases (solid lines). More specifically, the bias used for Y (simulating the RO bias) varies linearly between pressure levels as:

- 5 –5 to 2 % from 1000 to 800 hPa
- 2 to –4 % from 800 to 650 hPa
- 4 to 5 % from 650 to 500 hPa
- 5 to –11 % from 500 to 300 hPa

The bias used for Z (simulating the RS bias) varies linearly between pressure levels as:

- 10 3 to 1 % from 1000 to 700 hPa
- 1 to –8 % from 700 to 500 hPa
- 8 to –50 % from 500 to 300 hPa

The respective bias is added to both Y and Z when the data are created from the True profiles:

- $X = \text{True} + X_{\text{err}}$; corresponds to ERA
- 15 $Y = \text{True} + Y_{\text{err}}$; corresponds to RO
- $Z = \text{True} + Z_{\text{err}}$; corresponds to RS

We use these specified biased data sets to compute error variances via the 2CH method. Results are shown in Fig. 14, with the results of the real data in the top row (a–c), and the results of the simulated bias data in the bottom row (d–f).

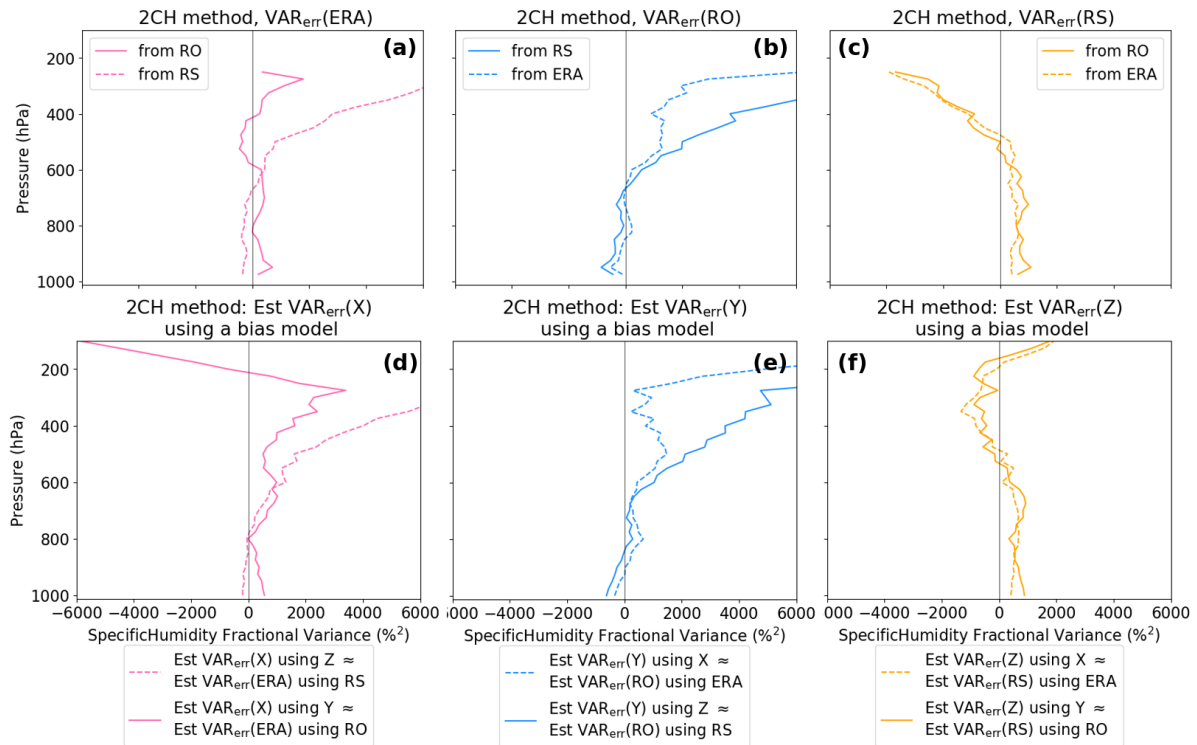


Figure 14. 2CH method error variances for ERA, RO, and RS (top row) and for simulated data using the specified empirical bias profiles (bottom). Correlation between X and Z errors is zero for this experiment.

The error variances of the simulated biased data sets (bottom row) are quite similar to the error variances estimated with the real data (top row), indicating that biases are largely responsible for the results using real data and how they vary from the 3CH method results.

6 Summary and conclusions

- 5 In this study we compared two methods for estimating the error variances of multiple data sets, the three-cornered hat (3CH) and two-cornered hat (2CH) methods. Using a simulated data set in which we could vary the degree of correlation between two data sets as well as specifying bias errors, we examined the sensitivity of the 3CH and 2CH methods to random and bias errors. For the error model, we added known random or bias errors to 1460 specific humidity profiles (considered truth) obtained from the ERA-Interim reanalysis (ERA) over a subtropical radiosonde station in Japan. We compared the effect of neglecting various error covariance and other error terms in the 3CH and 2CH methods on the estimated error variances and standard deviations.
- 10 We also considered the effect of a finite sample size on the estimates by repeating the calculations using a subset of 146 of the total 1460 profiles. We found that the 3CH method was less sensitive to the neglected error terms for various random error

correlations than the 2CH method. We also showed that the effect of bias errors on one of the data sets had a relatively small effect on the 3CH method, but produced much larger errors in the 2CH method.

We also compared the 3CH and 2CH methods using real radiosonde (RS), radio occultation (RO), and ERA data. We find that the 3CH method produces more consistent and accurate results than the 2CH method when using real data. The 2CH method produced very different estimates of the error variance of ERA depending on which observational data set (e.g. RS or RO) was used in the comparison. Using an empirical bias model based on observed RS and RO difference from ERA during 2007, we showed that these differences in error variance estimates were likely caused by different biases in the RS and RO data. The effect of bias errors is shown to give unrealistic results using the 2CH method.

Code availability. Code will be made available by the author upon request.

10 *Data availability.* Data can be made available from authors upon request.

Appendix A: Derivation of the 2CH method

In the 2CH method, sums and differences of two data sets X and Z are used to derive the error variances of X and Z .

$$X = \text{True} + X_{\text{err}} \quad (\text{A1})$$

$$Z = \text{True} + Z_{\text{err}} \quad (\text{A2})$$

$$15 \quad (X + Z)^2 = 4\text{True}^2 + 4\text{True} (X_{\text{err}} + Z_{\text{err}}) + (X_{\text{err}} + Z_{\text{err}})^2 \quad (\text{A3})$$

$$(\text{A4})$$

Equation (A3) is summed over all the data pairs to get

$$\frac{1}{n} \sum (X + Z)^2 = 4 \frac{1}{n} \sum \text{True}^2 + \frac{1}{n} \sum [(X_{\text{err}} + Z_{\text{err}})^2 + 4\text{True} (X_{\text{err}} + Z_{\text{err}})] \quad (\text{A5})$$

20 Defining the following expressions:

$$M(X) = \frac{1}{n} \sum X$$

$$M(X, Y) = M(X \cdot Y) = \frac{1}{n} \sum XY$$

Eq. (A5) becomes

$$25 \quad \begin{aligned} MS(X + Z) = & 4MS(\text{True}) + \text{VAR}_{\text{err}}(X) + \text{VAR}_{\text{err}}(Z) \\ & + 2\text{COV}_{\text{err}}(X, Z) + 4M(\text{True}, X_{\text{err}} + Z_{\text{err}}) \end{aligned} \quad (\text{A6})$$

We then subtract Z from X and square the difference to get

$$\text{MS}(X - Z) = \text{VAR}_{\text{err}}(X) + \text{VAR}_{\text{err}}(Z) - 2\text{COV}_{\text{err}}(X, Z) \quad (\text{A7})$$

Finally, we solve for $\text{MS}(\text{True})$ by subtracting Eq. (A7) from Eq. (A6)

$$4\text{MS}(\text{True}) = \text{MS}(X + Z) - \text{MS}(X - Z) - 4\text{COV}_{\text{err}}(X, Z) - 4\text{M}(\text{True}, X_{\text{err}} + Z_{\text{err}}) \quad (\text{A8})$$

5 By squaring the expression $X = (\text{True} + X_{\text{err}})$ we get the exact expression for the $\text{VAR}_{\text{err}}(X)$

$$\text{VAR}_{\text{err}}(X) = \text{MS}(X) - \text{MS}(\text{True}) - 2\text{M}(\text{True}, X_{\text{err}}) \quad (\text{A9})$$

and substituting for $\text{MS}(\text{True})$ from Eq. (A8) gives

$$\begin{aligned} \text{VAR}_{\text{err}}(X) = & \text{MS}(X) - \frac{1}{4}[\text{MS}(X + Z) - \text{MS}(X - Z)] \\ & - 2\text{M}(\text{True}, X_{\text{err}}) + \text{COV}_{\text{err}}(X, Z) + \text{M}(\text{True}, X_{\text{err}} + Z_{\text{err}}) \end{aligned} \quad (\text{A10})$$

Similarly, we obtain

$$\begin{aligned} \text{VAR}_{\text{err}}(Z) = & \text{MS}(Z) - \frac{1}{4}[\text{MS}(X + Z) - \text{MS}(X - Z)] \\ & - 2\text{M}(\text{True}, Z_{\text{err}}) + \text{COV}_{\text{err}}(X, Z) + \text{M}(\text{True}, X_{\text{err}} + Z_{\text{err}}) \end{aligned} \quad (\text{A11})$$

We note that the top lines in Eqs. (A10) and (A11) may be written as $\text{VAR}_{\text{err}}(X) = \text{MS}(X) - \text{M}(XZ)$ and $\text{VAR}_{\text{err}}(Z) = \text{MS}(Z) - \text{M}(XZ)$, which are the forms used by Stoffelen (1998) and Vogelzang et al. (2011).

Author contributions. Both authors contributed equally to the ideas and conceptual development. The first author computed the results.

Competing interests. The authors declare that they have no conflict of interest.

15 *Acknowledgements.* The authors were supported by NSF-NASA grant AGS-1522830. We thank Shay Gilpin for Fig. 4 and the two reviewers for their comments on the original draft. We thank Eric DeWeaver (NSF) and Jack Kaye (NASA) for their long-term support of COSMIC.

References

- Anthes, R. and Rieckh, T.: Estimating observation and model error variances using multiple data sets, *Atmos. Meas. Tech. Discuss.*, <https://doi.org/10.5194/amt-2017-487>, in review, 2018.
- Braun, J., Rocken, C., and Ware, R.: Validation of line-of-sight water vapor measurements with GPS, *Radio Sci.*, 36, 459–472, 2001.
- 5 Chen, S.-Y., Huang, C.-Y., Kuo, Y.-H., and Sokolovskiy, S.: Observational Error Estimation of FORMOSAT-3/COSMIC GPS Radio Occultation Data, *Mon. Wea. Rev.*, 139, 853–865, <https://doi.org/10.1175/2010MWR3260.1>, 2011.
- Collard, A. D. and Healy, S. B.: The combined impact of future space-based atmospheric sounding instruments on numerical weather-prediction analysis fields: A simulation study, *Quart. J. Roy. Meteor. Soc.*, 129, 2741–2760, <https://doi.org/10.1256/qj.02.124>, 2003.
- Dee, D. P., Uppala, S. M., Simmons, A. J., Berrisford, P., Poli, P., Kobayashi, S., Andrae, U., Balmaseda, M. A., Balsamo, G., Bauer, P.,
10 Bechtold, P., Beljaars, A. C. M., van de Berg, L., Bidlot, J., Bormann, N., Delsol, C., Dragani, R., Fuentes, M., Geer, A. J., Haimberger, L., Healy, S. B., Hersbach, H., Hólm, E. V., Isaksen, I., Kållberg, P., Köhler, M., Matricardi, M., McNally, A. P., Monge-Sanz, B. M., Morcrette, J.-J., Park, B.-K., Peubey, C., de Rosnay, P., Tavolato, C., Thépaut, J.-N., and Vitart, F.: The ERA-Interim reanalysis: configuration and performance of the data assimilation system, *Quart. J. Roy. Meteor. Soc.*, 137, 553–597, <https://doi.org/10.1002/qj.828>, 2011.
- Desroziers, G. and Ivanov, S.: Diagnosing and adaptive tuning of observation-error parameters in a variational assimilation, *Quart. J. Roy. Meteor. Soc.*, 127, 1433–1452, <https://doi.org/10.1002/qj.49712757417>, 2001.
- 15 Ekstrom, C. R. and Koppang, P. A.: Error Bars for Three-Cornered Hats, *IEEE Trans. Ultrason. Ferroelect. Freq. Contr.*, 53, 876–879, <https://doi.org/10.1109/TUFFC.2006.1632679>, 2006.
- Gray, J. E. and Allan, D. W.: A method for estimating the frequency stability of an individual oscillator, Atlantic City, New Jersey, May 29–31, 1974.
- 20 Griggs, E., Kursinski, E., and Akos, D.: An investigation of GNSS atomic clock behaviour at short time intervals, *GPS Solut.*, 18, 443–452, <https://doi.org/10.1007/s10291-013-0343-7>, 2014.
- Griggs, E., Kursinski, E., and Akos, D.: Short-term GNSS satellite clock stability, *Radio Sci.*, 50, 813–826, <https://doi.org/10.1002/2015RS005667>, 2015.
- Gruber, A., Su, C.-H., Zwieback, S., Crow, W., Dorigo, W., and Wagner, W.: Recent advances in (soil moisture) triple collocation analysis, *Int. J. Appl. Earth Obs. and Geoinf.*, 45, 200–211, <https://doi.org/10.1016/j.jag.2015.09.002>, 2016.
- 25 Ho, S.-P., Kuo, Y.-H., Schreiner, W., and Zhou, X.: Using SI-traceable Global Positioning System radio occultation measurements for climate monitoring, *Bull. Amer. Meteor. Soc.*, 91, S36–S37, 2010a.
- Ho, S.-P., Zhou, X., Kuo, Y.-H., Hunt, D., and Wang, J.-H.: Global evaluation of radiosonde water vapor systematic biases using GPS radio occultation from COSMIC and ECMWF analysis, *Remote Sensing*, 2, 1320–1330, <https://doi.org/10.3390/RS2051320>, 2010b.
- 30 Kuo, Y.-H., Wee, T.-K., Sokolovskiy, S., Rocken, C., Schreiner, W., Hunt, D., and Anthes, R. A.: Inversion and error estimation of GPS radio occultation data, *J. Meteor. Soc. Japan*, 82, 507–531, 2004.
- Kursinski, E. R., Hajj, G. A., Schofield, J. T., Linfield, R. P., and Hardy, K. R.: Observing Earth’s atmosphere with radio occultation measurements using the Global Positioning System, *J. Geophys. Res.*, 102, 23 429–23 465, <https://doi.org/10.1029/97JD01569>, 1997.
- Luna, D., Pérez, D., Cifuentes, A., and Gómez, D.: Three-Cornered Hat Method via GPS Common-View Comparisons, *IEEE Trans. Instrument. Measure.*, 66, 2143–2147, <https://doi.org/10.1109/TIM.2017.2684918>, 2017.
- 35 O’Carroll, A. G., Eyre, J. R., and Saunders, R. S.: Three-way error analysis between AATSR, AMSR-E, and in situ sea surface temperature observations, *J. Atmos. Oceanic Tech.*, 25, 1197–1207, <https://doi.org/10.1175/2007JTECHO542.1>, 2008.

- Rieckh, T., Anthes, R., Randel, W., Ho, S.-P., and Foelsche, U.: Evaluating tropospheric humidity from GPS radio occultation, radiosonde, and AIRS from high-resolution time series, *Atmos. Meas. Tech. Discuss.*, <https://doi.org/10.5194/amt-2017-486>, accepted, 2018.
- Riley, W. J.: <http://www.wiley.com/3-CornHat.htm>, 2003.
- Roebeling, R. A., Wolters, E. L. A., Meirink, J. F., and Leijnse, H.: Triple collocation of summer precipitation retrievals from SEVIRI over Europe with gridded rain gauge and weather radar data, *Journal of Hydrometeorology*, 13, 1552–1566, <https://doi.org/10.1175/JHM-D-11-089.1>, 2012.
- Stoffelen, A.: Toward the true near-surface wind speed: Error modeling and calibration using triple collocation, *J. Geophys. Res.*, 103, 7755–7766, <https://doi.org/10.1029/97JC03180>, 1998.
- Su, C.-H., Ryu, D., Crow, W. T., and Western, A. W.: Beyond triple collocation: Applications to soil moisture monitoring, *J. Geophys. Res.*, 119, 6419–6439, <https://doi.org/10.1002/2013JD021043>, 2014.
- Valty, P., de Viron, O., Panet, I., Camp, M. V., and Legrand, J.: Assessing the precision in loading estimates by geodetic techniques in Southern Europe, *Geophys. J. Int.*, 194, 1441–1454, <https://doi.org/10.1093/gji/ggt173>, 2013.
- Vogelzang, J., Stoffelen, A., Verhoef, A., and Figa-Saldaña, J.: On the quality of high-resolution scatterometer winds, *J. Geophys. Res.*, 116, <https://doi.org/10.1029/2010JC006640>, 2011.
- von Engel, A. and Nedoluha, G.: Retrieval of temperature and water vapor profiles from radio occultation refractivity and bending angle measurements using an Optimal Estimation approach: a simulation study, *Atmos. Chem. Phys.*, 5, 1665–1677, <https://doi.org/10.5194/acp-5-1665-2005>, 2005.
- Wang, B.-R., Liu, X.-Y., and Wang, J.-K.: Assessment of COSMIC radio occultation retrieval product using global radiosonde data, *Atmos. Meas. Tech.*, 6, 1073–1083, <https://doi.org/10.5194/amt-6-1073-2013>, 2013.